Research Article

Representative volume element based micromechanical modelling of rod shaped glass filled epoxy composites

Aanchna Sharma[1] · Yashwant Munde[2] · Vinod Kushvaha[1]

Received: 19 October 2020 / Accepted: 20 January 2021 / Published online: 28 January 2021

Abstract
In this study, Representative Volume Element based micromechanical modeling technique has been implemented to assess the mechanical properties of glass filled epoxy composites. Rod shaped glass fillers having an aspect ratio of 80 were used for preparing the epoxy composite. The three-dimensional unit cell model of representative volume element was prepared with finite element analysis tool ANSYS 19 using the periodic square and hexagonal array with an assumption that there is a perfect bonding between the filler and the epoxy matrix. Results revealed that the tensile modulus increases and Poisson's ratio decreases with increase in the volume fraction of the filler. To study the effect of filler volume fraction, the pulse echo techniques were used to experimentally measure the tensile modulus and Poisson's ratio for 5% to 15% volume fraction of the filler. A good agreement was found between the RVE based predicted values and the experimental results.

Keywords Glass filled composites · Representative volume element · Finite element analysis · Micromechanical modeling · Poisson's ratio · Tensile modulus

1 Introduction

Polymer matrix and the fiber reinforcement when blended together give result to a material commonly known as fiber reinforced polymer composite. In recent years, polymer composites have made remarkable progress and are being substantially used as a potential alternative to conventionally used structural materials. These composites are being extensively utilized in various engineering applications due to the excellent combination of properties that they possess [1, 2]. Polymer composites are well known for their high strength to weight ratio, high fracture toughness, resistance to corrosion, acoustic damping and thermal insulation [3–5]. Unlike traditional fiber reinforced composites, particulate polymer composites consist of a polymeric matrix reinforced with a dispersed phase in the form of particles like silica, zirconia, alumina, mica etc. The key advantage of such composites lies in the fact that they are easy to manufacture, structurally simpler and macroscopically isotropic [6]. In order to achieve a desired performance of the composite materials, it's imperative to appropriately select the shape, size and the amount of fiber reinforcement which is used to strengthen the matrix [7, 8]. Many researchers have made efforts to quantify the performance of polymer composites in terms of their mechanical response under different loading conditions. Kushvaha et al. [9] studied experimentally the effect of using different shapes and volume fraction of glass fillers on the mechanical properties of the resulting polymer composites. They used bisphenol epoxy as the matrix and glass particles of three different shapes viz. spherical, flake and rod in a volume fraction of 5%, 10% and 15% respectively as reinforcement. Results of their study highlighted the best performance of rod shaped

✉ Vinod Kushvaha, vinod.kushvaha@iitjammu.ac.in | [1]Department of Civil Engineering, Indian Institute of Technology, Jammu, India. [2]Department of Mechanical Engineering, MKSSS's Cummins College of Engineering for Women, Pune, Maharashtra 411052, India.

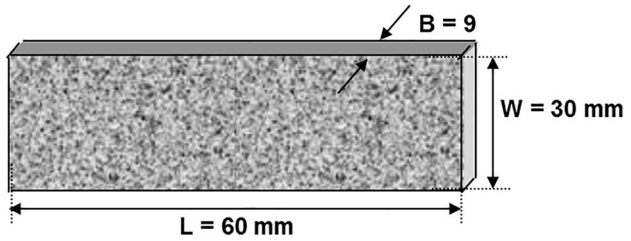

Fig. 1 Schematic diagram of the composite specimen used

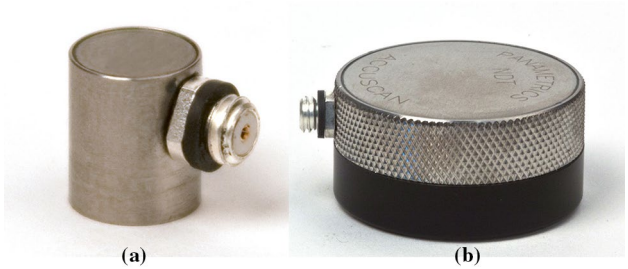

Fig. 2 Ultrasonic transducer **a** for longitudinal wave, **b** for shear wave

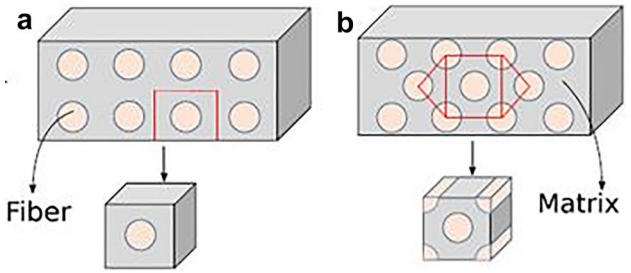

Fig. 3 RVE Models with packaging patterns **a** square **b** hexagonal [35]

Table 1 Elastic properties of the constituent materials

Constituent	Density (g/cm^3)	Tensile modulus (GPa)	Poisson's ratio
Filler: rod shaped glass	2.500	70.00	0.220
Matrix: Epoxy	1.146	3.99	0.370

fillers at a volume fraction of 15% under quasi-static loading conditions. A few more studies indicate that the variations in the aspect ratio of the filler material has a pronounced effect on the Young's modulus and in-plane shear modulus which in turn affects the overall performance of the composite material [10–12]. The intricacies that exist in carrying out the complex experimental procedures to highlight the efficacy of using polymer composites have resulted in the development of various analytical and numerical models [13–15]. Acoustic emission is another technique used to study and investigate the mechanical behaviour and various failure modes of composites. Sause et al. [16] used acoustic emission technique to quantify failure under mode-I loading conditions in carbon/glass reinforced epoxy composites. Fotouhi et al. [17] successfully used acoustic emission analysis to characterize the damage caused to glass reinforced epoxy composites under different modes of loading. Devireddy et al. [18] used micromechanical approach to evaluate the elastic and thermal properties of glass reinforced polymer composites. They came up with a finite element model based on the technique of Representative Volume Element (RVE) with a hexagonal and square packing geometry and implemented it using a code in ANSYS. RVE was developed by considering the different cross-sections of the glass fiber. Properties of interest were obtained by applying the periodic boundary conditions to the developed RVE. Later the same properties were calculated by using some analytical models like Halpin–Tsai, rule of mixture and Chawla model. Results found corresponding to both the models were in good agreement. Patnaik et al. [19] successfully predicted the micromechanical properties of glass reinforced epoxy composites by using a finite element model based on Representative Area Element (RAE) approach. Seidel and Lagoudas [20] used the approach of micromechanical analysis to determine the elastic properties of polymer composites reinforced with carbon nanotube. Liu and Chen [21] applied a 3-dimensional nanoscale RVE approach to find the material constants of carbon nanotube reinforced polymer composites under different loading conditions. Sakaguchi et al. [22] used the approach of representative volume element based on micromechanics to predict the elastic modulus and shrinkage of polymer matrix composites. Riano et al. [23] made use of RVE based finite element model to develop a mesoscopic model that could predict the mechanical behavior of fiber reinforced polymer composites. Another research group [24] applied RVE based numerical model to predict the mechanical properties of rice husk particulate reinforced epoxy composites. They used seven different analytical models to compare the results of numerical and analytical approach with the experimental values and the results were in good agreement with each other. Annapragada et al. [25] developed a micromechanics model to predict the mechanical and thermal properties of particulate composites. They used the methodology of RVE based on random packing geometry and predicted the mechanical properties using finite element model while the thermal properties were predicted using a finite volume approach.

The developed model was also capable of capturing the stress-bridging phenomenon of the particulates. Melro et al. [26] applied a constitutive damage model on epoxy composites to predict their damage response under varying load conditions. Considering the random distribution of fibers, different RVE's were considered and periodic boundary conditions were applied. The proposed model was successfully used to study the damage initiation and its propagation in the epoxy-fiber interface along with longitudinal shear and transverse tension. Adeniyi et al. [27] used a numerical homogenization approach to predict the elastic properties of polystyrene composites reinforced with sisal fibers. They developed a RVE with hexagonal packing and considered the circular cross-section of the sisal fiber followed by a finite element analysis using ABAQUS. Volume fraction of the reinforcing filler, the cross-sectional area and the RVE were found to significantly affect the mechanical response of polymer composites [28–30]. Another study [31] indicated that the larger sized RVE resulted in closer bulk properties of composites to the experimental values compared to the ones obtained from smaller sized RVE. Increase in tensile modulus with increase in the filler loading was reported by Munde et al. [32] for Sisal/PP and Johnson et al. for [33] for sansevieria cylindrical/vinyl ester composite. In this view, the present study focuses on developing a three-dimensional unit cell model of RVE using the finite element analysis approach in ANSYS. For evaluating the efficacy of the RVE based micromechanical model, predicted tensile modulus and Poisson's ratio of rod shaped glass-filled epoxy composites are compared with the experimental results reported elsewhere [9]. The novelty of the present research lies in the fact that for the first time a very simplistic approach has been used to model the complex behavior of rod-shaped glass filler reinforced particulate polymer composites. Hereafter, the paper is organized as, Sect. 2: materials and methods, Sect. 3: results and discussions followed by Sect. 4: conclusions.

2 Materials and method

2.1 Experimental procedure

For fabricating the sheets of glass filled epoxy composites, Bisphenol epoxy resin and an amine based hardener were used for the matrix phase. The density of the epoxy resin and the hardener was 1130 kg/m^3 and 961 kg/m^3 respectively. Rod shaped glass fillers having an average length and diameter of 800 µm and 10 µm respectively with a density of 2500 kg/m^3 were procured from Fiberglass Supply, USA. These rod shaped glass fillers were added to the epoxy resin and hence served as the reinforcement phase in the resulting composite. The mixture of epoxy and the glass fillers was completely degassed and uniform filler dispersion was ensured. Just before pouring the prepared mixture in the mold, hardener was added in stoichiometric proportion. After curing the prepared sheets for a week at room temperature, they were demolded and machined into rectangular specimens of 60 mm × 30 mm × 9 mm (refer to Fig. 1). In

Table 2 RVE model's symmetric boundary conditions

Displacement	Load case		
	1	2	3
u (X_0, X_1)	(1,0)	(0,0)	(0,0)
v (Y_0, Y_1)	(0,0)	(1,0)	(0,0)
w (Z_0, Z_1)	(0,0)	(0,0)	(1,0)

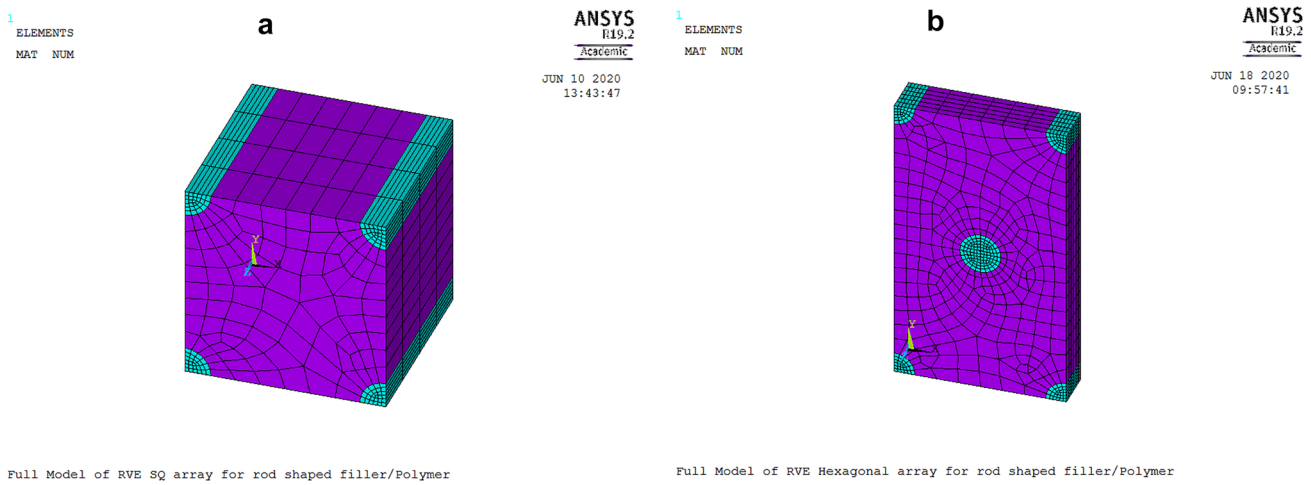

Fig. 4 A three dimensional meshed model of RVE for **a** square and **b** hexagonal packaging patterns

order to measure the elastic properties of the prepared composite specimens, ultrasonic non-destructive testing was performed. Following the procedure of ultrasonic pulse echo method, two transducers procured from Panametrics Engineering Pvt. Ltd. were used. Transducers V129 RM, 10 MHz (see Fig. 2a) and V156 RM, 5 MHz (see Fig. 2b) were used for receiving and transmitting the longitudinal and shear wave respectively. These ultrasonic transducers were then further connected with an oscilloscope and signal analyzer that helped in determining the longitudinal (C_l) and shear wave speed (C_s) at distinct locations of the prepared specimen. After calculating the material density (ρ), Poisson's ratio (γ) and elastic modulus (E) of the resulting composite were obtained using the following equations.

$$C_l = \sqrt{\frac{E(1-\gamma)}{\rho(1+\gamma)(1-2\gamma)}} \tag{1}$$

$$C_s = \sqrt{\frac{E}{2\rho(1+\gamma)}} \tag{2}$$

2.2 Numerical method: micromechanical modeling

To forecast the mechanical characteristics of fiber/filler reinforced polymer matrix composites, micromechanical modeling is one of the most effective techniques. This technique is widely implemented with different finite element analysis tools to analyze the failure of composites.

Table 3 Results of mesh convergence study for square RVE

Square RVE for rod shaped filler reinforced polymer			
No. of divisions through depth, fiber & matrix portion along length and width respectively	4,8	8,16	8,24
V_f (%)	No. of Elements		
5	836	10,536	24,728
10	1348	12,760	28,080
15	1528	14,624	32,000
	Transverse Modulus (MPa)		
5	4608.82	4608.40	4608.29
10	5108.85	5108.30	5109.03
15	5662.09	5663.81	5662.37
	Poisson's ratio		
5	0.3604	0.3604	0.3604
10	0.3517	0.3517	0.3517
15	0.3430	0.3431	0.3430

Table 4 Results of mesh convergence study for hexagonal RVE

Hexagonal RVE for rod shaped filler reinforced polymer			
No. of divisions through depth, fiber & matrix portion along l ength and width respectively	4,8	8,16	8,24
V_f (%)	No. of elements		
5	2464	19,768	45,768
10	2496	19,920	45,856
15	2584	21,264	49,504
	Transverse modulus (MPa)		
5	4586.06	4584.24	4585.74
10	5077.94	5079.52	5079.64
15	5453.14	5454.30	5455.31
	Poisson's ratio		
5	0.3605	0.3605	0.3605
10	0.3512	0.3512	0.3512
15	0.3442	0.3442	0.3442

In the present work, RVE based micromechanical modeling technique has been implemented to investigate the mechanical characteristics of rod shaped glass filler reinforced epoxy composites. RVE of 1 mm^2 square area and 1 mm depth was prepared and the overall composite was assumed to be unidirectional (UD) [34]. Selecting the smallest possible size of RVE supports the assumption that the composites can be treated as UD lamina. There are certain ways to idealize the cross section of lamina and define the packaging of fillers in the matrix. Here, two types of RVE's are considered based on the square and hexagonal assortments (see Fig. 3) which are generally preferred arrangements in the micromechanical modeling. The inputs for the current analysis are specified in Table 1 i.e. elastic properties of constituent materials (rod shaped glass fillers and epoxy matrix).

The finite element analysis tool ANSYS 19 has been used to prepare three dimensional RVE model. In this modeling, assumption was made that filler and the polymer matrix have seamless interfacial bonding and they are homogeneous and isotropic in nature. The Eqs. (3) and (4) were used for the preparation of RVE model for square and hexagonal packaging respectively. Based on the known values of geometry dimensions (length (a_1), width (a_2) and height (a_3)) and filler volume fraction (V_f), the diameter of the filler (d_f) was calculated. A selection of SOLID 186 type of element is conformed because this element has 20 nodes along with three degrees of freedom per node. It supports for layered structural solid and allows to model the layered thick shells or solids and reveals quadratic displacement behavior. This element also supports for large deflections which aid to apply displacement boundary conditions of surfaces of RVE. The mapped meshing is implemented to acquire a meshed model of RVE. In this, initially number of divisions through thickness, fiber and matrix chosen are 4, 6, and 8 respectively. Later the divisions are increased till the resultant values of solution get converged. The meshed model of RVE for square and hexagonal packaging pattern is shown in Fig. 4.

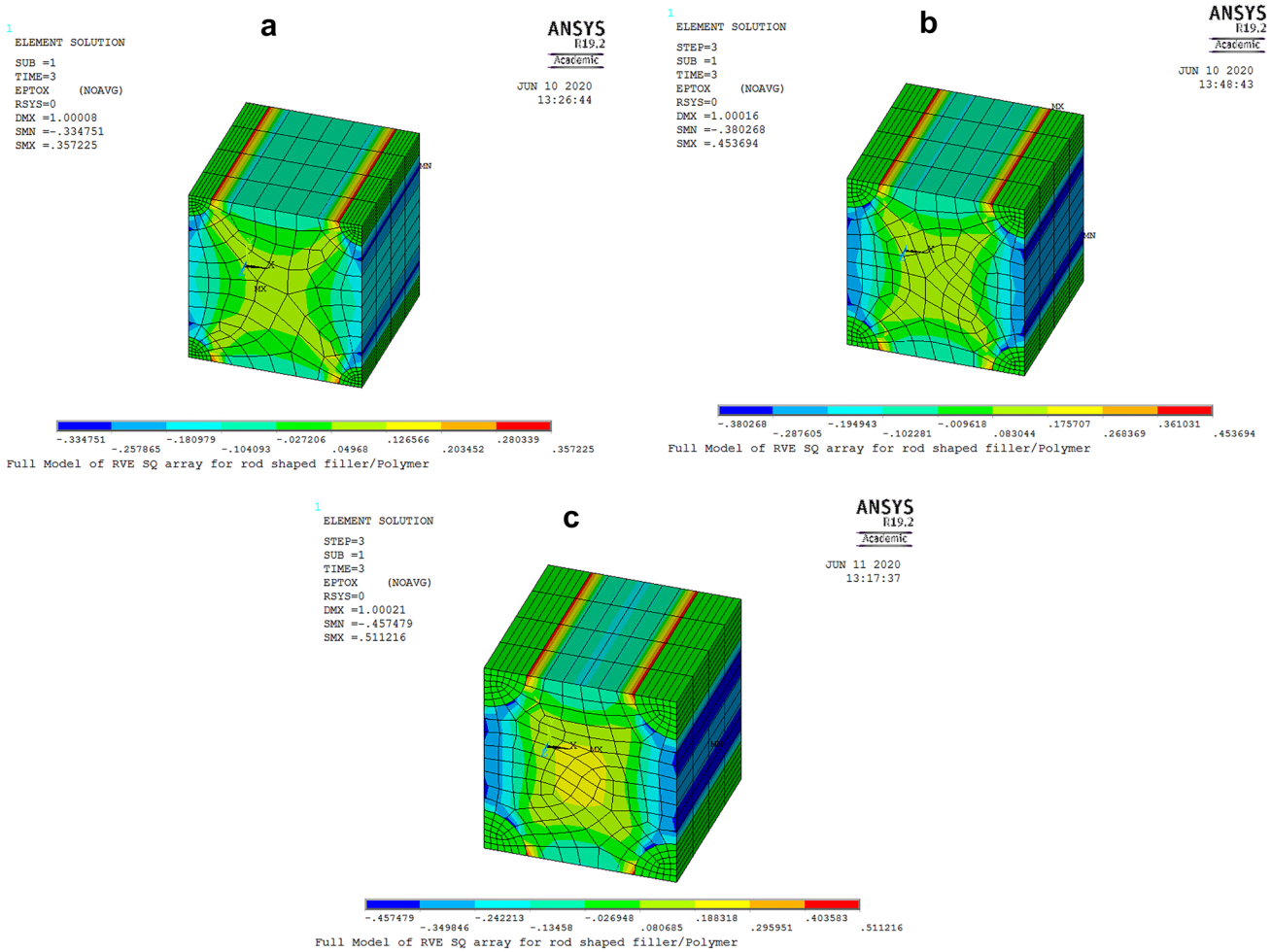

Fig. 5 Strain (X direction) contour plots at 5, 10 and 15% V_f of filler with square array

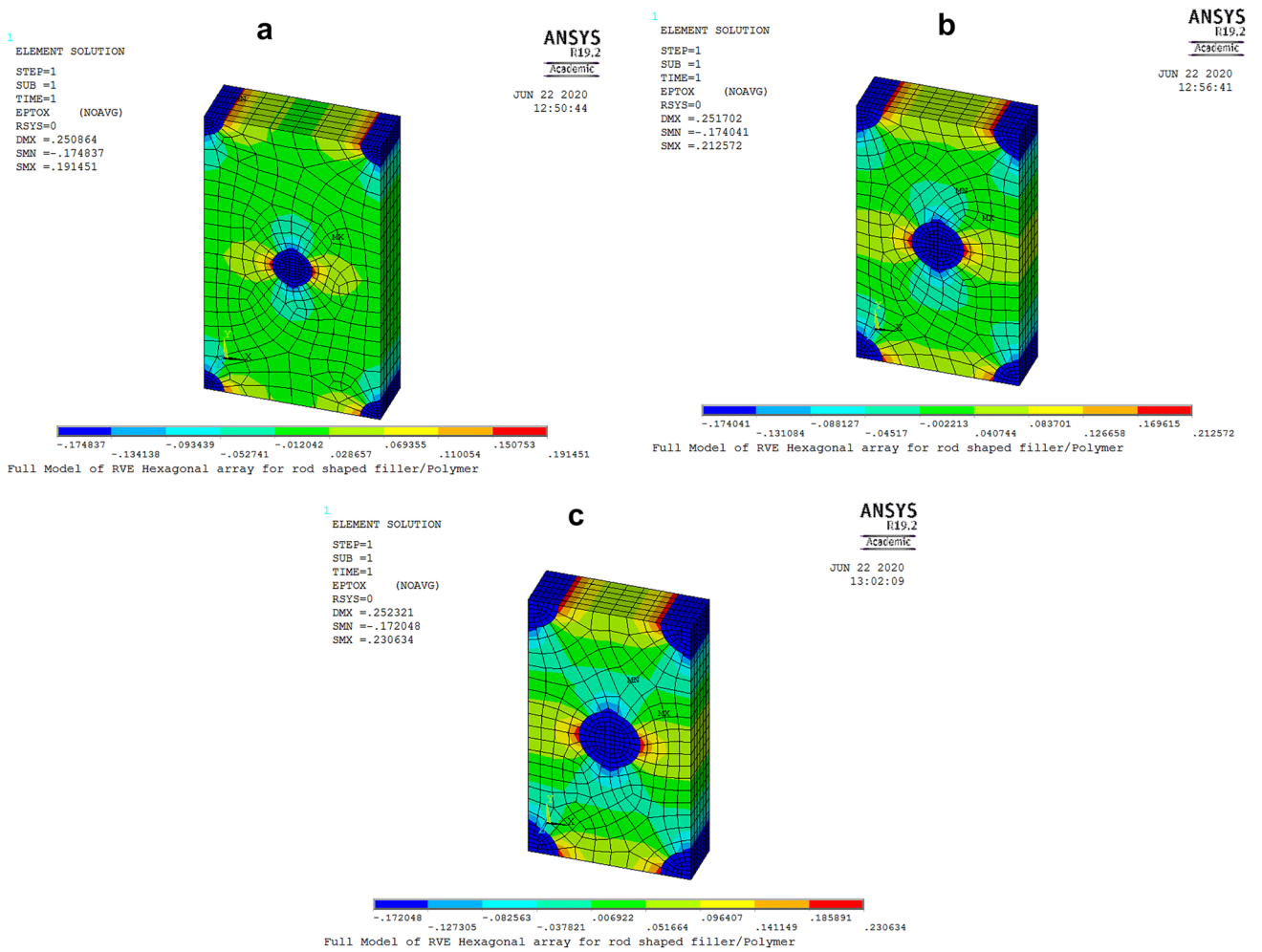

Fig. 6 Strain (X direction) contour plots at 5, 10 and 15% V_f of filler with hexagonal array

$$V_f = \frac{a_1\left(\frac{\pi}{4}\right)d_f^2}{4a_1a_2a_3} \tag{3}$$

where $a_1 = a_2 = a_3 = 1$ mm

$$V_f = \frac{2a_1\left(\frac{\pi}{4}\right)d_f^2}{a_1a_2a_3} \tag{4}$$

where $a_1 = 1$ mm, $a_2 = 4\,a_1$ and $a_3 = a_2 \tan(60^0)$.

The symmetric boundary conditions (BC's) for the meshed RVE model were set as shown in Table 2. The displacement BC's were applied on each of the surface of model for all three load cases. The u, v and w are the values of displacement defined on each surface of RVE along the principal directions of the geometry as X, Y and Z respectively. The X_0, X_1, Y_0, Y_1, Z_0, Z_1 are the left, right, top, bottom, back and front surface of RVE model respectively.

After applying the boundary conditions, the model was solved with three load cases to get the elemental stresses and strains values. Then the average stresses and average strains of unit cell were calculated by using Eqs. (5) and (6).

$$\overline{\sigma}_{ij} = \frac{1}{V}\int_V \sigma_{ij}dV \tag{5}$$

$$\overline{\varepsilon}_{ij} = \frac{1}{V}\int_V \varepsilon_{ij}dV \tag{6}$$

The stress–strain relationship is represented by Eq. (7). The elements of the stiffness tensor (C_{ij}) matrix were calculated by taking a ratio of average stress to the average strain. The stiffness matrix elemental values were further

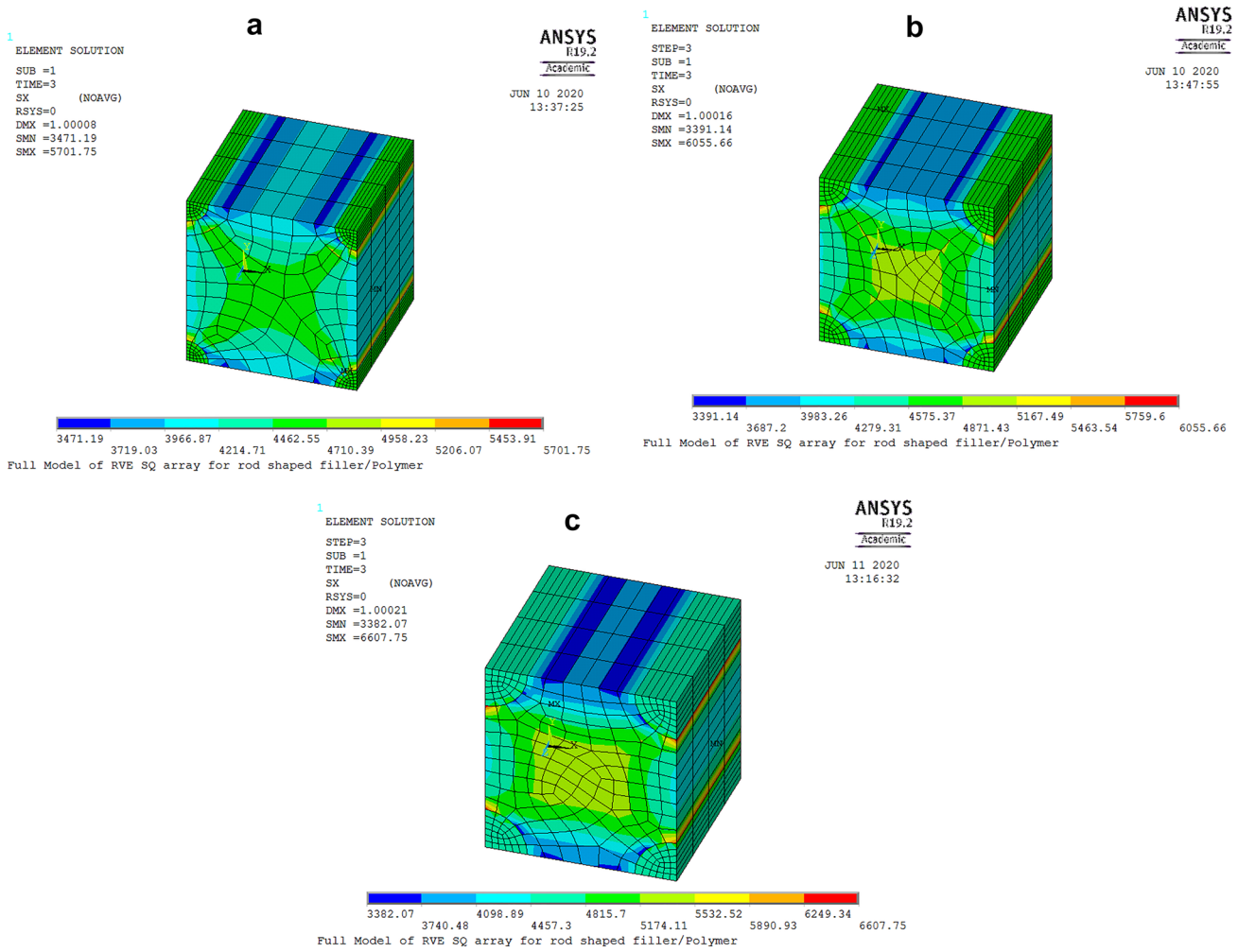

Fig. 7 Stress (X direction) contour plots at 5, 10 and 15% V_f of filler with square array

used to estimate the mechanical properties as modulus of elasticity (E_1 and E_2), in-plane shear modulus (G_{12}) and Poisson's ratio (γ_{12}) using equations from (7) to (11).

$$\{\sigma_i\} = [C_{ij}]\{\varepsilon_i\} \tag{7}$$

where, i, j = 1, 2, 3, 4, 5, 6

$$E_1 = C_{11} - \frac{2C_{12}^2}{(C_{22} + C_{23})} \tag{8}$$

$$E_2 = \frac{[2C_{11}(C_{22} + C_{23}) - 2C_{12}^2](C_{22} - C_{23})}{(C_{11}C_{22} - C_{12}^2)} \tag{9}$$

$$G_{12} = \frac{1}{2}(C_{22} - C_{23}) \tag{10}$$

$$\gamma_{12} = \frac{C_{12}}{(C_{22} + C_{23})} \tag{11}$$

3 Results and discussion

Model of RVE was generated for the rod shaped glass filler-epoxy composites using ANSYS 19.0. Mesh convergence study was also performed, results for which are shown in Tables 3 and 4. For each model, the numbers of elements were increased by reducing the mesh size. But the results analogue to each model were nearly same.

The modulus of elasticity/tensile modulus of all the compositions (i.e. 5, 10, 15% V_f) was estimated from the stress and strain values at each of the considered load case and the known material properties. The contour plots of strain for square array and hexagonal array are shown in Figs. 5 and 6 respectively. In Fig. 5, strain along x direction

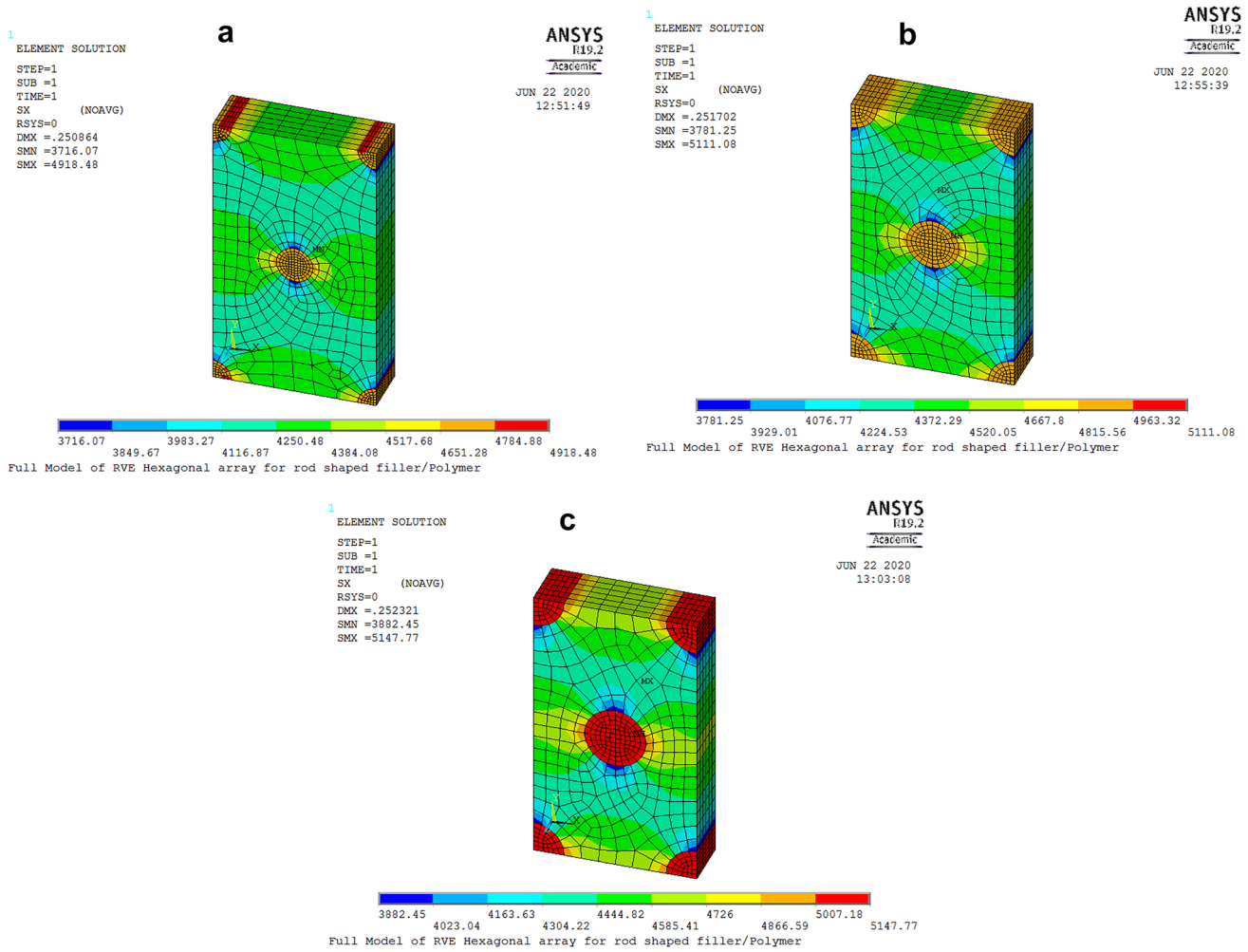

Fig. 8 Stress (X direction) contour plots at 5, 10 and 15% V_f of filler with hexagonal array

Table 5 Comparison of predicted and experimental values of the tensile modulus

V_f of filler (%)	Tensile modulus (MPa)			Percentage error in the predicted values (%)	
	Square array RVE	Hexagonal array RVE	Experimental	Square array RVE	Hexagonal array RVE
5	4608.29	4585.74	4620.08	0.25	0.74
10	5109.03	5079.64	5080.02	0.57	0.01
15	5662.37	5455.31	5670.04	0.13	3.78

shows a unit value for all three compositions which confirm that the BC's were applied correctly.

The corresponding stress contour plots for square array and hexagonal array patterns are depicted in Figs. 7 and 8 respectively. From the values of these stresses, a stiffness tensor followed by the tensile modulus of the composite has also been calculated.

The tensile longitudinal modulus of rod shaped glass filler-epoxy composites was estimated for different volume fractions of the filler. The appraisal of the tensile modulus predicted by RVE methods with experimental results is tabulated in Table 5. The tensile modulus increases with increase in filler loading from 5 to 15% throughout. This is because of incorporation of stiffer fiber in a polymer matrix. The tensile modulus predicted by RVE methods

Table 6 Comparison of predicted and experimental values of the Poisson's ratio

V_f of filler (%)	Poisson's ratio			Percentage error in the predicted values (%)	
	Square array RVE	Hexagonal array RVE	Experimental	Square array RVE	Hexagonal array RVE
5	0.3604	0.3605	0.3602	0.05	0.08
10	0.3517	0.3512	0.3601	2.33	2.47
15	0.3430	0.3442	0.3502	2.05	1.71

has shown a good agreement with the experimental values. The largest percentage deviation of predicted tensile modulus from the experimental values was observed to be 3.78%.

The ratio of contracted transverse strain to extended longitudinal strain for applied force gives the Poisson's ratio. The Poisson's ratio of the overall composites was estimated for each of the filler composition. It reveals that the decay in Poisson's ratio is observed with increase in filler content. This endorsed the increase in resistance for deformation and reduction in the elasticity of material. The deviation of the Poisson's ratio predicted by RVE methods from experimental results is minimal which is clear from the values tabulated in Table 6.

4 Conclusions

The current research work assessed the mechanical elastic properties of the rod shaped glass filler-epoxy composites with different filler volume fraction by using the approach of micromechanical modeling. A finite element analysis tool, ANSYS 19 was successfully used to model square and hexagonal packing patterned three dimensional RVE models to evaluate the mechanical elastic properties. Tensile modulus estimated by using the RVE based micromechanical approach has shown a maximum deviation of 3.78% with the experimental results. RVE model prediction has promising closeness with the experimental values with a maximum deviation of 2.47% for Poisson's ratio. The proposed methodology can further be applied on different polymer composite materials such as long fiber reinforced and woven fiber reinforced, to get an insight into the mechanical behavior of these composites with limited experimentation. The interface model in 3D micromechanical modeling will further help to analyze and understand interfacial strength properties of composites.

Acknowledgments The authors acknowledge the financial support received from the Ministry of Education (MoE), India and the seed grant received by IIT Jammu.

Compliance with ethical standards

Conflict of interest The authors declare that they have no conflict of interest.

References

1. Hassanzadeh-Aghdam M-K, Ansari R, Darvizeh A (2019) Multi-stage micromechanical modeling of effective elastic properties of carbon fiber/carbon nanotube-reinforced polymer hybrid composites. Mech Adv Mater Struct 26:2047–2061. https://doi.org/10.1080/15376494.2018.1472336
2. Kushvaha V, Branch A, Tippur H (2014) Effect of Loading Rate on Dynamic Fracture Behavior of Glass and Carbon Fiber Modified Epoxy. In: Song B, Casem D, Kimberley J (eds) Dynamic Behavior of Materials, vol 1. Springer International Publishing, Berlin, pp 169–176
3. Kushvaha V, Tippur H (2013) Effect of Filler Particle Shape on Dynamic Fracture Behavior of Glass-Filled Epoxy. In: Chalivendra V, Song B, Casem D (eds) Dynamic Behavior of Materials, vol 1. Springer, New York, pp 513–522
4. Bacarreza O, Abe D, Aliabadi MH, Kopula Ragavan N (2013) Micromechanical modeling of advanced composites. J Multiscale Model. https://doi.org/10.1142/S1756973712500059
5. Hemath M, Mavinkere Rangappa S, Kushvaha V, Dhakal HN, Siengchin S (2020) A comprehensive review on mechanical, electromagnetic radiation shielding, and thermal conductivity of fibers/inorganic fillers reinforced hybrid polymer composites. Polym Compos 41(10):3940–3965
6. Bucevac D (2014) 7—Heat treatment for strengthening silicon carbide ceramic matrix composites. In: Low IM (ed) Advances in Ceramic Matrix Composites. Woodhead Publishing, Cambridge. https://doi.org/10.1533/9780857098825.1.141

7. Fu S-Y, Feng X-Q, Lauke B, Mai Y-W (2008) Effects of particle size, particle/matrix interface adhesion and particle loading on mechanical properties of particulate–polymer composites. Compos B Eng 39:933–961. https://doi.org/10.1016/j.compositesb.2008.01.002
8. Sharma A, Kushvaha V (2020) Predictive modelling of fracture behaviour in silica-filled polymer composite subjected to impact with varying loading rates using artificial neural network. Eng Fract Mech 239:107328. https://doi.org/10.1016/j.engfracmech.2020.107328
9. Kushvaha V, Tippur H (2014) Effect of filler shape, volume fraction and loading rate on dynamic fracture behavior of glass-filled epoxy. Compos B Eng 64:126–137. https://doi.org/10.1016/j.compositesb.2014.04.016
10. Laws N, McLaughlin R (1979) The effect of fibre length on the overall moduli of composite materials. J Mech Phys Solids 27:1–13. https://doi.org/10.1016/0022-5096(79)90007-3
11. Tandon GP, Weng GJ (1984) The effect of aspect ratio of inclusions on the elastic properties of unidirectionally aligned composites. Polym Compos 5:327–333. https://doi.org/10.1002/pc.750050413
12. Wang J, Pyrz R (2004) Prediction of the overall moduli of layered silicate-reinforced nanocomposites—part II: analyses. Compos Sci Technol 64:935–944. https://doi.org/10.1016/S0266-3538(03)00025-3
13. Zhong Y, Tran LQN, Kureemun U, Lee HP (2017) Prediction of the mechanical behavior of flax polypropylene composites based on multi-scale finite element analysis. J Mater Sci 52:4957–4967. https://doi.org/10.1007/s10853-016-0733-7
14. Sharma A, Subramaniyan AK, Kushvaha V (2020) Effect of aspect ratio on dynamic fracture toughness of particulate polymer composite using artificial neural network. Eng Fract Mech 228:106907. https://doi.org/10.1016/j.engfracmech.2020.106907
15. Kushvaha V, Kumar SA, Madhushri P, Sharma A (2020) Artificial neural network technique to predict dynamic fracture of particulate composite. J Compos Mater. https://doi.org/10.1177/0021998320911418
16. Sause MGR, Müller T, Horoschenkoff A, Horn S (2012) Quantification of failure mechanisms in mode-I loading of fiber reinforced plastics utilizing acoustic emission analysis. Compos Sci Technol 72:167–174. https://doi.org/10.1016/j.compscitech.2011.10.013
17. Fotouhi M, Ahmadi Najafabadi M (2014) Investigation of the mixed-mode delamination in polymer-matrix composites using acoustic emission technique. J Reinf Plastics Compos 33:1767–1782. https://doi.org/10.1177/0731684414544391
18. Devireddy SBR, Biswas S (2014) Effect of fiber geometry and representative volume element on elastic and thermal properties of unidirectional fiber-reinforced composites. J Compos 2014:1–12. https://doi.org/10.1155/2014/629175
19. Patnaik A, Kumar P, Biswas S, Kumar M (2012) Investigations on micro-mechanical and thermal characteristics of glass fiber reinforced epoxy based binary composite structure using finite element method. Comput Mater Sci 62:142–151. https://doi.org/10.1016/j.commatsci.2012.05.020
20. Seidel GD, Lagoudas DC (2006) Micromechanical analysis of the effective elastic properties of carbon nanotube reinforced composites. Mech Mater 38:884–907. https://doi.org/10.1016/j.mechmat.2005.06.029
21. Liu YJ, Chen XL (2003) Evaluations of the effective material properties of carbon nanotube-based composites using a nanoscale representative volume element. Mech Mater 35:69–81. https://doi.org/10.1016/S0167-6636(02)00200-4
22. Sakaguchi RL, Wiltbank BD, Murchison CF (2004) Prediction of composite elastic modulus and polymerization shrinkage by computational micromechanics. Dent Mater 20:397–401. https://doi.org/10.1016/j.dental.2003.11.003
23. Riaño L, Belec L, Joliff Y (2016) Validation of a Representative Volume Element for unidirectional fiber-reinforced composites: Case of a monotonic traction in its cross section. Compos Struct 154:11–16. https://doi.org/10.1016/j.compstruct.2016.07.020
24. Saigal A, Pochanard P (2019) The application of a representative volume element (RVE) Model For The Prediction Of Rice Husk particulate-filled polymer composite properties. Mater Sci Appl 10:78. https://doi.org/10.4236/msa.2019.101008
25. Annapragada SR, Sun D, Garimella SV (2007) Prediction of Effective Thermo-Mechanical Properties of Particulate Composites. Am Soc Mech Eng Dig Collect. https://doi.org/10.1115/IMECE2006-14720
26. Melro AR, Camanho PP, Andrade Pires FM, Pinho ST (2013) Micromechanical analysis of polymer composites reinforced by unidirectional fibres: part II Micromechanical analyses. Int J Solids Struct 50:1906–1915. https://doi.org/10.1016/j.ijsolstr.2013.02.007
27. Adeniyi AG, Adeoye SA, Onifade DV, Ighalo JO (2019) Multi-scale finite element analysis of effective elastic property of sisal fiber-reinforced polystyrene composites. Mech Adv Mater Struct. https://doi.org/10.1080/15376494.2019.1660016
28. Adeniyi AG, Adeoye SA, Ighalo JO, Onifade DV (2020) FEA of effective elastic properties of banana fiber-reinforced polystyrene composite. Mech Adv Mater Struct. https://doi.org/10.1080/15376494.2020.1712628
29. Islam MDR, Pramila A (1999) Thermal Conductivity of Fiber Reinforced Composites by the FEM. J Compos Mater. https://doi.org/10.1177/002199839903301803
30. Raju B, Hiremath SR, Roy Mahapatra D (2018) A review of micromechanics based models for effective elastic properties of reinforced polymer matrix composites. Compos Struct 204:607–619. https://doi.org/10.1016/j.compstruct.2018.07.125
31. Valavala PK, Odegard GM, Aifantis EC (2009) Influence of representative volume element size on predicted elastic properties of polymer materials. Modell Simul Mater Sci Eng 17:045004. https://doi.org/10.1088/0965-0393/17/4/045004
32. Munde YS, Ingle RB, Siva I (2019) Effect of sisal fiber loading on mechanical, morphological and thermal properties of extruded polypropylene composites. Mater Res Exp 6:085307. https://doi.org/10.1088/2053-1591/ab1dd1
33. Johnson DJ, Arumugaprabu V, Munde YS (2019) Constitutive models to predict the mechanical performance of sansevieria cylindrica reinforced vinyl ester composite. Mater Res Exp 6:095310. https://doi.org/10.1088/2053-1591/ab2e90
34. Raj R, Thakur DG (2016) Micromechanical modelling of fibre reinforced metal matrix composites subjected to longitudinal tensile loading. Int J Mater Eng Innov 7:56–79. https://doi.org/10.1504/IJMATEI.2016.077317
35. Munde YS, Ingle RB, Shinde AS, Irulappasamy S (2020) Micromechanical modelling and evaluation of pineapple leaves fibre (PALF) composites through representative volume element Method. Springer, Berlin, pp 249–264. https://doi.org/10.1007/978-981-15-1416-6_12